Physica B 500 (2016) 59–65

Contents lists available at ScienceDirect

Physica B

journal homepage: www.elsevier.com/locate/physb

Thermal phase transition in artificial spin ice systems induces the formation and migration of monopole-like magnetic excitations

Alejandro León

Facultad de Ingeniería, Universidad Diego Portales, Ejército 441, Santiago, Chile

ARTICLE INFO

Article history:
Received 7 August 2015
Received in revised form
2 July 2016
Accepted 11 July 2016
Available online 15 July 2016

Keywords:
Magnetic monopoles
Spin ice
Thermal phase transition

ABSTRACT

Artificial spin ice systems exhibit monopole-like magnetic excitations. We develop here a theoretical study of the thermal phase transition of an artificial spin ice system, and we elucidate the role of the monopole excitations in the transition temperature. The dynamics of the spin ice is described by an efficient model based on cellular automata, which considers both thermal effects and dipolar interactions. We have established the critical temperature of the phase transition as function of the magnetic moment and the energy barrier of reversion. In addition, we predict that thermal gradients in the system induce the motion of elementary excitations, which could permit to manipulate monopole-like states.

1. Introduction

Artificial spin ice systems are highly frustrated arrangements of nanomagnets, where the localized magnetic moments interact through dipolar fields. The equilibrium magnetic configuration in artificial spin ice systems resembles the order of hydrogen and oxygen atoms in another frustrated system, namely water crystals. The experimental and theoretical research focused on artificial spin ice systems has grown considerably in recent years, due to both the possible technological applications and the interesting physical effects involved [1–9]. In the first experimental investigations, the artificial spin ice samples were composed of magnetic nanoislands with high reversal barriers (about $\sim 10^4$ K), and therefore thermal effects were not observed at room temperature. Interesting works have been published on thermal activation in artificial spin ice systems [10–17]. In a recent work, Kapaklis and colleagues studied experimentally thin films composed of few atomic monolayers [18]. The reversal barriers of their nanoislands are well below the room temperature and therefore their experiments are ideal to study thermal fluctuations. Moreover, when the temperature is increased, this system presents a transition from a frozen to a dynamic state; which is characterized by the emergence of localized excitations.

From the theoretical point of view, the existence of two types of elementary magnetic excitations, namely heavy and light monopoles, has been predicted in the context of magnetic reversions in artificial spin ice systems [19]. In the one case, the magnetic inversion is accompanied by the appearance of static magnetic monopoles (heavy monopoles) and the absence of Dirac chains. In the second case, elemental magnetic excitations appear in the system and move long distances along the sample (light monopoles), giving rise to extensive Dirac chains during the magnetic reversion. In general, both types of excitations emerge artificial spin ice systems during the magnetic reversal.

In this work we study the dynamics of elementary monopoles-like excitations in a square array of nanomagnets, as function of the temperature and the magnetic properties of the individual components of the array. Our results show that the critical temperature of the phase transition strongly depends on the energy barrier for the reversion of the nanomagnets and on their magnetic moment. This study confirms the presence of two forms of elementary excitations (light and heavy monopoles) and its influence on the critical temperature of phase change. Furthermore, we found propagation of light monopoles driven by temperature gradients.

2. Frustrated cellular automata model and physical system

A cellular automaton (CA) is a mathematical structure used to model the dynamics of complex systems. It is formed by many simple entities that interact locally. A variety of models based on CA have been used to efficiently study problems in biology, physics, chemistry, engineering and material sciences [20,21]. They represent an excellent alternative to models based on differential equations and to Monte Carlo algorithms because they can simulate highly complex systems with a low computational cost. The first attempt to use CA in the study of magnetism was the model proposed by Vichniac [22], which was subsequently developed by Pomeau [23] and Hermann [24] and is termed the VPH model. This is being used to resolve an Ising type spin system. To avoid a

http://dx.doi.org/10.1016/j.physb.2016.07.012
0921-4526/

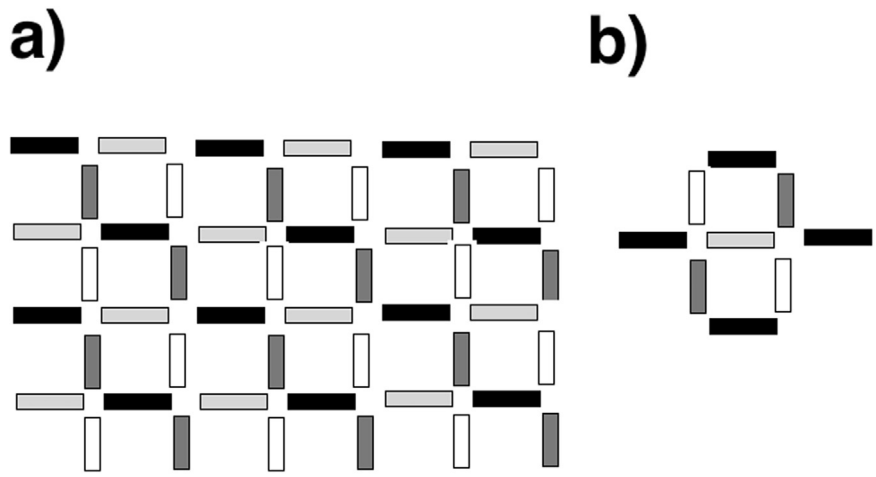

Fig. 1. (a) Square lattice of nanoislands. There are four different types of nanoislands in the lattice. (b) Each cell is surrounded by eight neighboring cells.

"feedback catastrophe", the automaton is updated in more than one step. The model functioned well at high temperatures ($T > T_C$), but failed at low temperatures. Subsequently, Ottavi et al. [25] used a microcanonical algorithm in a CA to resolve the Ising spin system. A determinist version of this model provided acceptable results at a low temperature [25]. Owing to the popularity of the different types of Monte Carlo algorithms used in problems associated with spins, the development of CA models for these systems did not continue. In this work we used a stochastic CA model, different from previous models, developed specifically to resolve the dynamic of frustrated spins in artificial spin ice systems. This model allows the simulation of spin ice systems efficiently. In our model, the cells represent nanoislands, and the local interaction among the cells is the dipolar effect. The state of the cells stands for the magnetic moment, and the evolution rule is obtained by local energy minimizations. This model is a variation of the numerical scheme proposed in Ref. [26], which has been compared and validated [27] with the experimental work of Mengotti et al. [8]. Fig. 1(a) shows a square lattice of nanoislands, where each cell represents an anisotropic magnet with form of a parallelepiped. The long axis of the parallelepiped is a preferred direction for its magnetization (easy axis), and therefore the localized moment takes only two possible orientations. Then, the orientations of the magnetization and the island (horizontal or vertical) defines four independent types of nanoislands in the system (see Fig. 1). In order to model the nonlocal dipolar interaction as the interaction between a cell and a few of its neighbors, we conducted a careful study considering a different number of neighbors. As a result of this study, we established that it is enough to consider the eight closest neighbors to each cell to recovery all the dynamic properties. Fig. 1(b) shows the configuration of the first neighbors that we consider.

The simulation scheme of the CA is summarized in the following steps:

- Each time step in the algorithm is divided into four stages.
- In each temporal step, a sequence of the four colors is chosen randomly.
- For every cell of a given color, we calculate the total energy as the sum of the energy associated to the external magnetic field and the dipolar field (up to eight neighbors). The magnetic moment of the nanoisland is reverted if its new energy is lower than the previous energy. If the energy is larger, the moment reversion occurs with a probability given by the Boltzmann distribution:
- The above step is repeated for the three remaining colors.
- The CA update finishes. This sequence represents the global update of the system.

The main difference of this model with a model kinetic Monte Carlo, is that in the CA, all nanoislands are inspected in a step of the algorithm (parallel upgrade), instead in the Monte Carlo approach, one generates a Markov chain of configurations using a pseudo-random number generator. We can also add that this algorithm satisfies detailed balance, because it is alternately updated on four sublattices [28–30].

We consider a square array of 7200 nanomagnets. The total lengths of the sample are $36\,\mu m \times 36\,\mu m$, and the distance between two adjacent nanomagnets (the lattice constant) is $a = 500 \rightarrow 700$ nm. Possible manufacturing imperfections of the film are taken into account using a variable magnetic moment within the lattice. Moreover, the magnetic moment of individual islands is defined by $m_0' = m_0\beta$, where β is a dimensionless Gaussian random variable with $\langle\beta\rangle = 1$ and standard deviation $s = \left(\left\langle\left(\beta - \langle\beta\rangle^2\right)\right\rangle\right)^{\frac{1}{2}}$.

Fig. 2(c) shows the color coding used in this work to represent the monopole-type elementary magnetic excitations. As we can see from this figure, the configuration of vertices are classified according to its energy. If each magnetic moment is interpreted as a bar with two magnetic charges at the ends ($+1$ and -1), we can evaluate the net charge, at each vertex, because the ends of the four bars converge. In a square lattice of magnets, the magnetic moments are ordered in minimum energy configurations, called "spin ice" (two in and two out), in analogy to the way the water crystallizes. In spin ice vertices, the total charge is zero. The first two rows of Fig. 2(c) correspond to spin ice configurations and hence they are energy minima. In the third and fourth rows, we can appreciate the violation of the rules of spin ice, leading to the appearance of magnetic excitations (monopoles). These monopoles can be positive or negative ($+2$ or -2). In the last row you can appreciate monopoles with value is $+4$ or -4, whose occurrence is unlikely in both the simulations and the experiment and that will not be considered in this study. In a previous result [19], it showed that the reversion dynamic presents two distinct mechanisms of magnetic reversion, with different elemental excitations for each mechanism. The first mechanism presents a reversion with the appearance of magnetic monopoles that do not move in the samples (heavy monopoles) and the absence of Dirac chains. In the other mechanism elemental magnetic excitations (light monopoles) appear that move great distances in the sample, giving rise to extensive Dirac chains during the magnetic

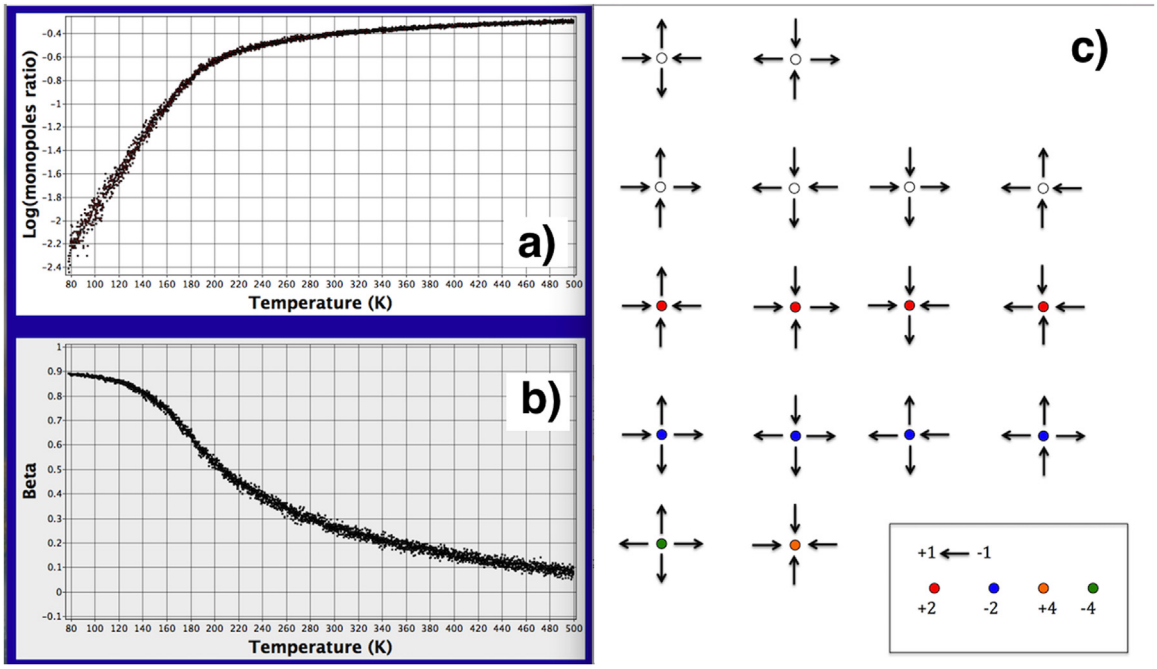

Fig. 2. (a) Logarithm of the total number of excitations as function of temperature. As this figure illustrates, the slope of the curve decreases for temperatures above a critical value, which is associated to the thermal phase transition. (b) Order parameter (Beta) as function of temperature. (c) Color scheme used along this work. Red vertex represent a positive magnetic monopole, while the blue vertex stand for negative monopoles. (For interpretation of the references to color in this figure caption, the reader is referred to the web version of this paper.)

reversion. The two kinds of monopoles (heavy and light) have magnetic charge of $+2$ or -2.

3. Critical temperature of the phase transition

Let us start studying the phase transition between the ordered and disordered states. We proceed is as follows: initially the system is at a temperature above room temperature without magnetic field. The temperature is decreased, and at each step of the algorithm we recorded the most relevant physical observables involved in the process. We can see in Fig. 2(c), the first two rows correspond to vertices spin ice type. In a completely random phase, the fraction of such vertexes is 0.375 (we denominate this value g_1). We will use this data to define the order parameter, as follows: the fraction of vertices spin ice type (N_{si}), above g_1 and divided by $(1-g_1)$ value, will be our order parameter. Mathematically, we have $Beta = \frac{N_{si}-g1}{1-g1}$. Thus, the order parameter will take the value zero, in a completely disordered phase and will take the value 1 in the ordered phase completely. Additionally, we will use the fraction of elementary excitations (monopoles), to verify the phase transition. This fraction is inversely proportional to order parameter beta. For the graphics remain clear, we show the logarithm of the fraction of elementary excitations (Fig. 2(a)). Fig. 3 shows the state of the system at different temperatures, which is characterized by the presence of magnetic monopoles and Dirac strings. The nanomagnets painted white, represent magnetic moment upward and to the right, while the nanomagnets painted black, represent magnetic moment down and to the left respectively. In this simulation, the values are: $a = 600$ nm, $s = 0.03$, $m_0 = 3{\cdot}10^6\,\mu_B$ and $B{=}0$. Furthermore, the relationship between the magnetic moment of each nanomagnet and the temperature is: $m(T) = m_0'\left(1-\frac{T}{T_0}\right)^{1/2}$, with $T_0 = 700$ K in this simulation. We define "energy barrier" for each nanomagnet, as the energy required to reverse the magnetic moment of each island. The value of the "energy barrier" in this simulation is $E_B = 200\ \mathrm{K}/k_B$. The initial temperature of the system was 500 K and it was decreased to 70 K, using steps of 0.05 K. We will call "Study 1" to this set of parameters. The logarithm of the ratio of monopoles (positive and negative) is shown in Fig. 2(a) and order parameter (Beta) as function of temperature is shown in Fig. 2(b).

The analysis of these results clearly indicates that the system changes from a disordered phase to an order phase when the temperature decreases. The critical temperature at which the phase transition occurs is $T_C = 190$ K (see Fig. 2(a) and (b)). It is interesting to note that the total magnetization of the sample has an initial value zero in the disordered state, remaining at this value in the ordered state. This is due to the ordered state, there is almost no vertices with elementary excitations (monopoles), and therefore the system has a majority of spin ice vertices, and therefore with null total magnetization. When inspecting the order parameter in Fig. 2(a) and (b), we can conclude that the system suffered a continuous phase transition of second order. It is known that the elementary excitations are divided into heavy monopoles and light monopoles [19]. The presence of a class of these excitations (heavy or light), or both types, depends on the energy barrier of reversion E_B, and the magnetic moment m_0 of each nanoisland [19]. For the values of the magnetic moment and the energy of reversal of the system shown in Fig. 3, only light monopole are present. In order to understand the effect of light and heavy monopoles in the phase transition, we studied the critical temperature as function of the magnetic moment and energy barrier of reversion, with the same parameters used in study 1. The results of this study are shown in Fig. 4.

As Fig. 4 illustrates, the critical temperature increases with the energy barrier of magnetic reversal. Also, when we increase the value of the magnetic moment of the nanoislands, an increase occurs in the phase change temperature. We incorporated a logarithmic trendline to display the kind of growth in temperature.

For values lower than 600 K in the energy barrier of magnetic reversal, in Fig. 4, the elementary excitations present are light

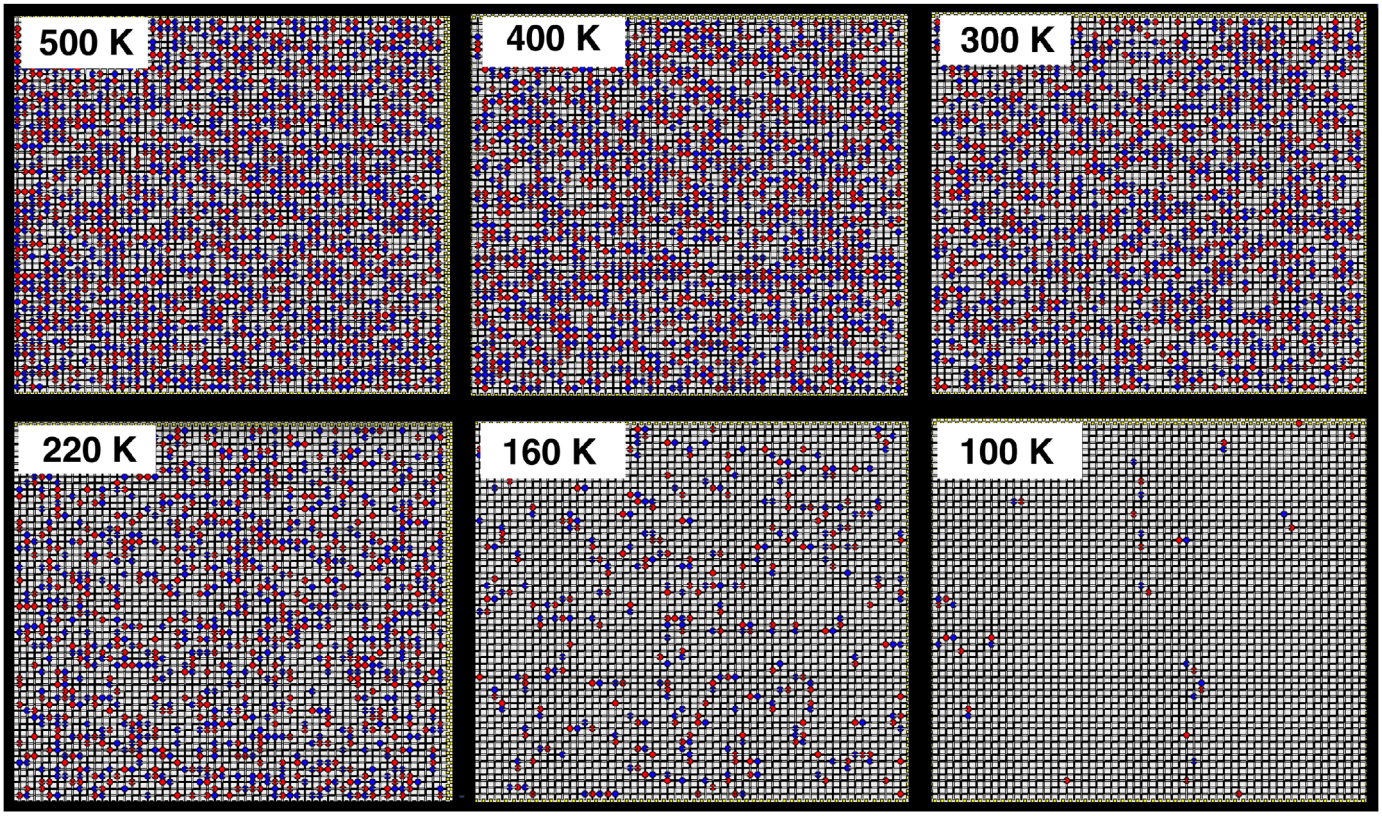

Fig. 3. Simulation of phase change from a disordered state to an ordered state. The black and white bars represent the magnets and its magnetic polarization state. Red and blue circles represent the magnetic monopoles. The nanomagnets painted white, represent magnetic moment upward and to the right, while the nanomagnets painted black, represent magnetic moment down and to the left respectively. (For interpretation of the references to color in this figure caption, the reader is referred to the web version of this paper.)

monopoles. In the disordered state, monopoles emerge, move and collide with other monopoles, disappearing and re-emerging elsewhere. In the ordered state, monopoles emerge and move until the system minimizes the energy locally and disappear. The behavior of heavy monopoles does not depend on the order of the system, and it is characterized by pairs of heavy monopoles with opposite charge appearing and disappearing in the same place. We can explain the slope of the curves in Fig. 4, with the two types of monopoles present in these artificial spin ice systems. In the first part of the curves (values less than 400 K), the slope is greater than on the right side, because the dynamics of elementary excitations is governed by light monopoles, and therefore a small variation in the value of the magnetic moment or reversal energy barrier, causes a major change in the temperature of phase change. In contrast, in the zone dominated by heavy monopoles (right side of Fig. 4), a change in the magnetic moment or energy barrier, causes a small change in the phase change temperature.

We conducted simulations to elucidate how the critical temperature depends on the separation distance between the nanoislands, with the same parameters used in study 1. Fig. 5 shows that the temperature decreases with larger separation distances. Our results are in agreement with experimental evidence [18]. When the separation distance between the nanomagnets increases the dipolar interaction decreases, causing disorder at lower temperatures. Furthermore, a study of the critical temperature, depending on the system size (number of magnets present in the array) was performed. We concluded from this study that the temperature does not depend on the size of the system.

An interesting result was obtained when we include an external magnetic field. The magnetic field makes an angle of 45° with respect to the horizontal direction (x-axis) and we have used

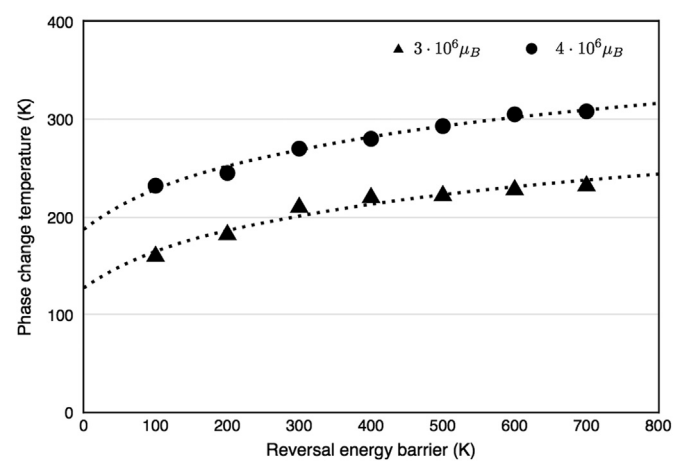

Fig. 4. Phase change temperature as function of the magnetic reversal energy. The upper curve represents the results obtained for a magnetic moment $m_0 = 4{\cdot}10^6\,\mu_B$ and the lower curve corresponds to a value of the magnetic moment $m_0 = 3{\cdot}10^6\,\mu_B$. Also incorporated in the graph, a logarithmic trendline for each case.

the same parameters used in study 1 and a magnetic moment $m_0 = 4{\cdot}10^6\,\mu_B$. We call "crossover temperature" (T_c), to the temperature at which the system passes from a disordered phase to an ordered phase in the presence of a magnetic field. Fig. 6 shows the crossover temperature as a function of the magnitude of the applied magnetic field; and the magnetization of the system for some field values. It can be seen that the crossover temperature, has two different behaviors. In the first case, when the magnetic field increases, the crossover temperature decreases. We can explain this behavior with the screening effect produced by the

magnetic field on the dipolar interaction between the nanomagnets. This shielding disfavors the magnetic ordered at high temperatures. When the magnitude of the field surpasses a threshold value, the effect is opposite to the previous. This is explained because the field does sort the system. It can be seen from magnetization curves that with increasing magnetic field, the system starts with a non-zero magnetization. Depending on the magnitude of the field, the magnetization becomes zero in the ordered state, (configuration spin ice of the minimum energy), or is magnetized in the ordered state, (configuration spin ice, with more energy). It is worth noting that the use of an external magnetic field allows one to control the crossover temperature. An interesting result of this part of the study is that since the application of an external field breaks time reversal symmetry, we expect a fundamental change in the type of crossover. However, this does not occur until a threshold field value, where the crossover as phase transition of second order behaves and the ordered and disordered states are presented. The sample has an initial magnetization in the disordered state, because the magnetic field monopoles migrate in the direction of the field (or contrary to direction of the field), magnetizing the sample. For fields above the threshold, the transition remains second order, but the ordered state, is now magnetic.

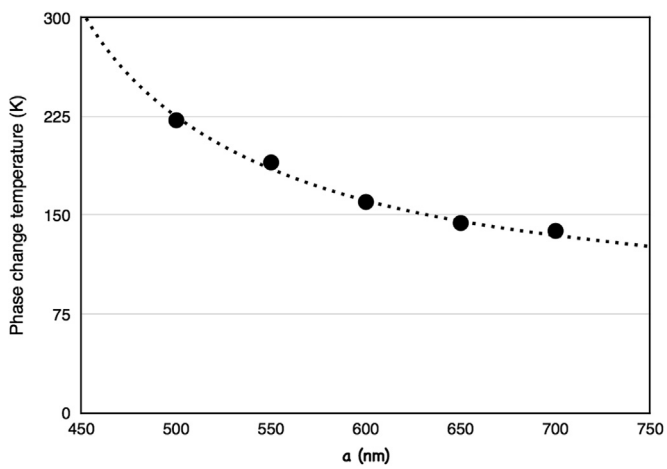

Fig. 5. Critical temperature as function of the distance between the nanomagnets.

4. Migrations of the elemental excitations

Finally, we study the propagation of magnetic monopoles induced by thermal gradients. The parameters involved in this study only allow the presence of light monopoles. The sample is initially magnetized with the nanomagnets to the right and up respectively. The central region of the array of nanomagnets is maintained at a temperature well below the phase change temperature. Thermal excitations are generated in two ways, the first consists to heat a thin strip of the right end of the square array and a thin strip of upper zone, as shown in Fig. 7(a) (red zone). This way of heating the system generates monopoles in the thin strip, but only positive monopoles move into the sample, (positive current of monopoles). The second way is to heat a thin strip around the contour of the sample. This generates a positive current of monopoles, moving down and to the left and a second negative current of monopoles, moving up and to the right, as shown in Fig. 7(b). The parameters for this simulation are: $a = 600$ nm, $s = 0.03$, $m_0 = 5{\cdot}10^6\,\mu_B$ $B = 0$. Further, $T_0 = 700$ K and the energy barrier for the inversion of the magnetic nanoislands is $E_B = 400\ \mathrm{K}/k_B$. The system remains at a constant temperature of 30 K and the ends are heated from 30 K to 120 K. It can be seen in Fig. 7(a), the positive monopole leave the hot zone and travel through the system at the other end. This mechanism would provide a controlled flow of a single class of magnetic excitations. In part (b) of Fig. 7, one can see a current of magnetic charges composed of positive and negative charges. Fig. 8 shows the ratio of magnetic charge depending on the temperature of the heated ends. The time period considered for the step of our algorithm is

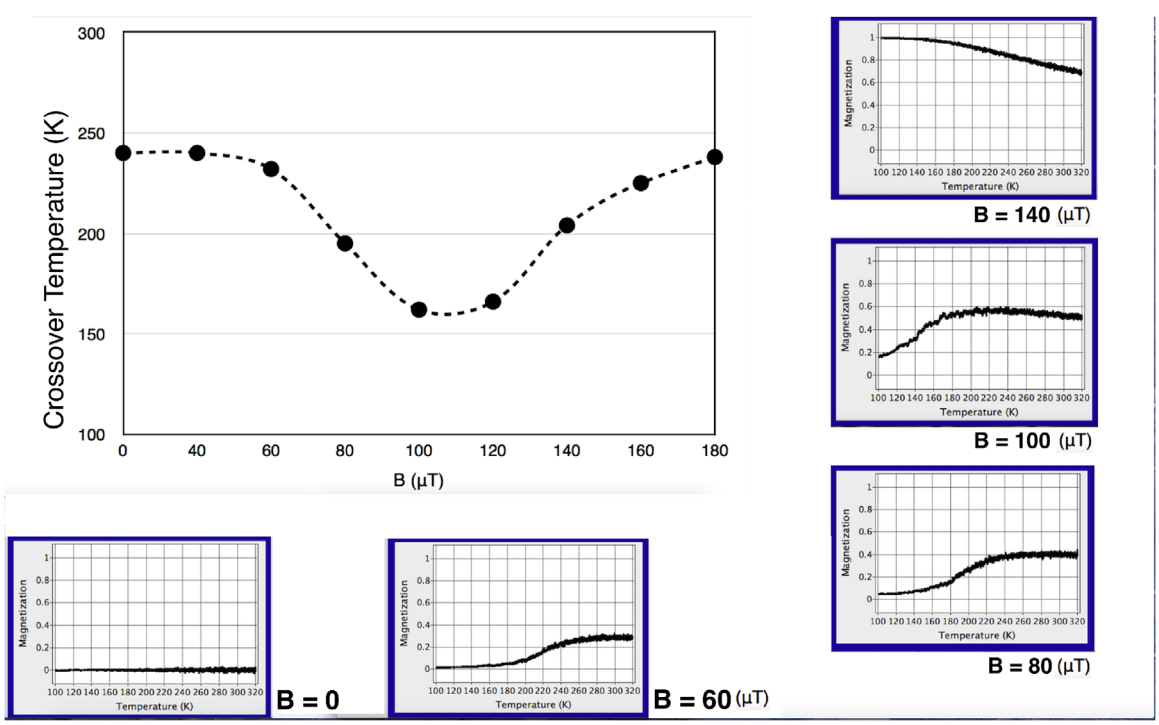

Fig. 6. Crossover temperature as a function of the magnitude of the applied magnetic field (in a direction of 45° to the horizontal). Small graphs show the magnetization, for some values of the magnetic field.

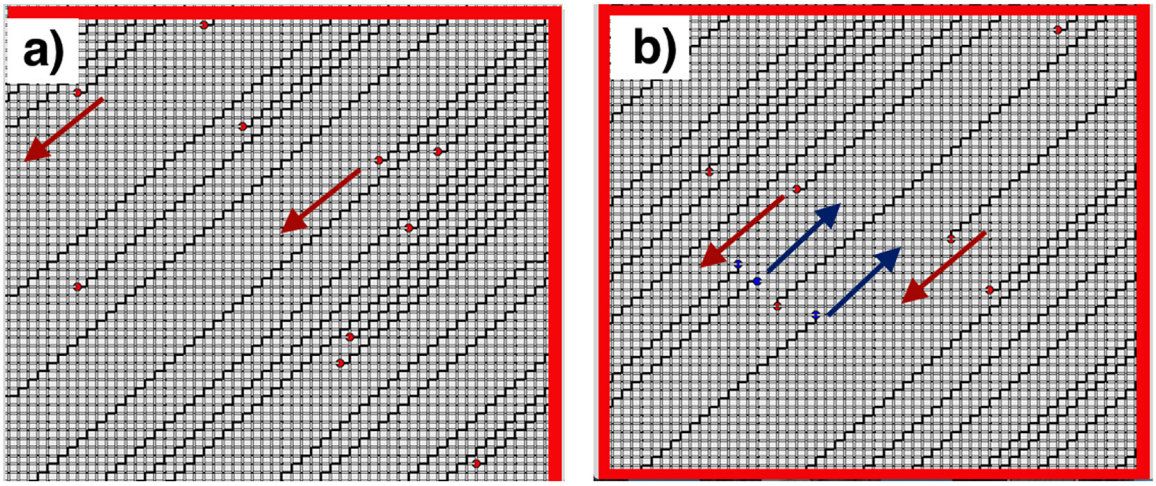

Fig. 7. Propagation of magnetic monopoles. (a) Positive magnetic current driven by thermal excitations in two hot edges. (b) Positive and negative magnetic current, triggered by thermal excitations in the four hot edges of the system.

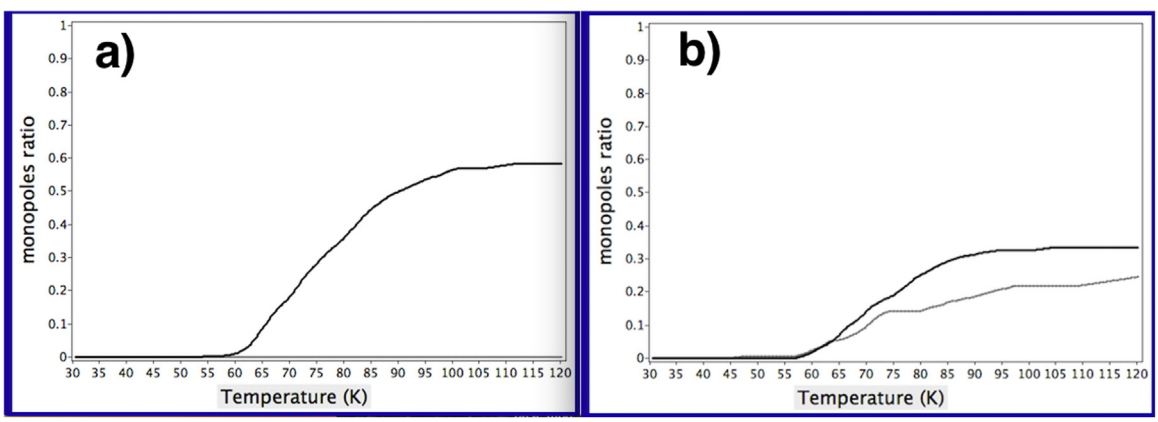

Fig. 8. Monopoles density as function of hot zone temperature, this ratio is defined as the number of monopoles divided by the total number of vertices. The black and gray curves stand for the positive and negative monopoles, respectively. (a) Two-sides heating. (b) Four-sides heating.

1×10^{-10} s [31]. This part of our study was performed with different time intervals for the increase in temperature. For the simulation shown in Figs. 7 and 8 the rate of increase in temperature was 1.5 K/ns.

5. Conclusion

This paper presents a numerical study of monopoles-like magnetic excitations in presence of thermal fluctuations. We described the system using an efficient model based on cellular automata that considers both the temperature of the system and dipolar interactions. Our results show a continuous second order transition from an ordered to a disordered state when the temperature increases. We found that the critical temperature of the phase transition strongly depends on the type of magnetic monopoles present in the system; which agrees with previous hypotheses[19] regarding the important role that the heavy and light monopoles play in the dynamics. When thermal gradients are applied on the sample, the magnetic charges propagate in a preferred direction fixed by the temperature profile. Hence, we can control the motion of magnetic charges, which could be a future tool for applications in information handling.

Acknowledgments

The author acknowledges the financial support of FONDECYT Program Grant 1151316.

References

[1] R.F. Wang, C. Nisoli, R.S. Freitas, J. Li, W. McConville, B.J. Cooley, M.S. Lund, N. Samarth, C. Leighton, V.H. Crespi, P. Schiffer, Nature 439 (2006) 303–306.
[2] E. Mengotti, L.J. Heyderman, A. Fraile Rodriguez, A. Bisig, L. Le Guyader, F. Nolting, H.B. Braun, Phys. Rev. B 78 (2008) 144402.
[3] A. Remhof, A. Schumann, A. Westphalen, H. Zabel, Phys. Rev. B 77 (2008) 134409.
[4] S. Ladak, D.E. Read, W. Branford, L.F. Cohen, New J. Phys. 13 (2011) 063032.
[5] P. Mellado, O. Petrova, Y.C. Shen, O. Tchernyshyov, Phys. Rev. Lett. 105 (2010) 187206.
[6] S. Ladak, D. Read, Tyliszczak, W.R. Branford, L.F. Cohen, New J. Phys. 13 (2011) 023023.
[7] S. Ladak, D. Read, G.K. Perkins, L.F. Cohen, W.R. Branford, Nat. Phys. 6 (2010) 359.
[8] E. Mengotti, L.J. Heyderman, A.F. Rodriguez, F. Nolting, R.V. Hugli, H.B. Braun, Nat. Phys. 7 (2011) 68–74.
[9] J.P. Morgan, A. Stein, S. Langridge, C.H. Marrows, New J. Phys. 13 (2011) 105002.
[10] Zhang, S.Ian Gilbert, Cristiano Nisoli, Gia-Wei Chern, Michael J. Erickson, Liam O'Brien, Chris Leighton, Paul E. Lammert, Vincent H. Crespi, Peter Schiffer, Nature 500 (2013) 553–557.
[11] C. Phatak, A.K. Petford-Long, O. Heinonen, M. Tanase, M. De Graef, Phys. Rev. B 83 (2011) 174431.
[12] S.D. Pollard, V. Volkov, Y. Zhu, Phys. Rev. B 85 (2012) 180402.
[13] J.P. Morgan, A. Stein, S. Langridge, C.H. Marrows, Nat. Phys. 7 (2011) 75–79.

[14] J.M. Porro, A. Bedoya-Pinto, A. Berger, P. Vavassori, New J. Phys. 15 (2013) 055012.
[15] A. Farhan, P.M. Derlet, A. Kleibert, A. Balan, R.V. Chopdekar, M. Wyss, L. Anghinolfi, F. Nolting, L.J. Heyderman, Nat. Phys. 9 (2013) 375–382.
[16] A. Farhan, P.M. Derlet, A. Kleibert, A. Balan, R.V. Chopdekar, M. Wyss, J. Perron, A. Scholl, F. Nolting, L.J. Heyderman, Phys. Rev. Lett. 111 (2013) 057204.
[17] D. Thonig, S. Reißaus, I. Mertig, J. Henk, J. Phys.: Condens. Matter 26 (2014) 266006.
[18] V. Kapaklis, U.B. Arnalds, A. Farhan, R.V. Chopdekar, A. Balan, A. Scholl, L. J. Heyderman, B. Hjörvarsson, Nat. Nanotechnol. 9 (2014) 514–519.
[19] A. León, Curr. Appl. Phys. 13 (2013) 2014–2018.
[20] D. Griffeath, C. Moore (Eds.), New Constructions in Cellular Automata, University Press, Oxford, 2003.
[21] A. León, Z. Barticevic, M. Pacheco, Solid State Commun. 152 (2012) 41–44.
[22] G.Y. Vichniac, Physica D 10 (1984) 96.
[23] Y. Pomeau, J. Phys. A 17 (1984) L-415.
[24] H.J. Hermann, J. Stat. Phys. 45 (1986) 145.
[25] H. Ottavi, O. Parodi, Europhys. Lett. 8 (1989) 741–746.
[26] A. León, Comput. Phys. Commun. 183 (2012) 10.
[27] A. León, J. Magn. Magn. Mater. 340 (2013) 120–126.
[28] P. Dai Pra, B. Scoppola, E. Scoppola, arXiv:1201.5756.
[29] C. Lancia, B. Scoppola. J. Stat. Phys. 153 (4), 641–653.
[30] E. Domany, W. Kinzel, Phys. Rev. Lett. 53 (1984) 311.
[31] S. Bedanta, W. Kleemann, Supermagnetism, J. Phys. D 42 (2008) 013001.